

NUMERICAL ANALYSIS OF BIOLOGICAL MATERIALS VITRIFICATION PROCESSES

Álisson Renan Stochero da Silva – alissonstochero@hotmail.com

Mario Henrique Macagnan – mhmac@unisinós.br

Jacqueline Biancon Copetti – jcopetti@unisinós.br

Karolyn Sassi Ogliari – karolyn@hemocord.com.br

Universidade do Vale do Rio dos Sinos, www.unisinós.br

R4 – Aplicações Industriais e Especiais

Resumo. *The cryopreservation of biological tissues and materials is a vast segment, present in several areas, such as medicine, pharmacology, biology, veterinary, bioengineering and biotechnology, among others. There are several researches in the fields of stem cells and assisted reproduction, sectors that are quite important and that still need more studies about the methods of cryopreservation, especially freezing protocols. Therefore, this work aims to carry out a brief systematic review of the ultra-fast freezing processes by vitrification and reproduce through CFD computational modeling the main cases found in the literature. It was studied the thermophysical phenomena involved during the dripping freezing process, such as cooling curves, solidification curves, contours of temperature and solidification, contact angle and droplet characteristic. Numerical simulations (CFD) of the drip freezing protocol were performed using the commercial software ANSYS Fluent® using three geometries with the same volume, 20 µL, and different contact angles $\theta = 45^\circ$, $\theta = 90^\circ$ and $\theta = 135^\circ$. The results shows that greater contact angles increases the cooling rate and the solidification rate, due to the bigger area of interface between the droplet and the substrate. It was found a value for the cooling rate for $\theta = 135^\circ$ of 1132.55 K/min, almost four times higher than $\theta = 45^\circ$ of 335.277 K/min. The CFD results presented in this work are in agreement with literature, being an excellent tool to study and investigate phenomena involving vitrification processes.*

Keywords: *Cryopreservation, Vitrification process, Computational fluid dynamics.*

1. INTRODUCTION

Cryo-refrigeration systems are present in the most diverse sectors of advanced technology, such as medicine, engineering, electronics and computer industry, aerospace and military sectors. In the context of health sciences, e.g. medicine, pharmacology and veterinary medicine, the cryopreservation segment stands out, which consists of conserving cellular materials in an environment with extremely low temperature for long periods and without significantly affect their viability after freezing. This field is quite wide, with strong application in freezing and preserving tissues and other biological materials, such as stem cells (obtained through blood and umbilical cord and bone marrow), semen (Le *et al.*, 2019; Li *et al.*, 2019; Cerdeira *et al.*, 2020), ovaries (Dalman *et al.*, 2017), embryos (Santin *et al.*, 2009), among others.

In the cryopreservation process, samples pass by three main stages, such as material preparation, freezing and storage. The freezing and storage of the materials are done through contact with a refrigerant fluid at an extremely low temperature. Nitrogen is generally used, available in abundance in the atmosphere in its natural gaseous state, due to its characteristics and properties, with a wide working range, with an approximate operating temperature between 43 and 126 K (liquid state), being an inert gas, odorless, tasteless and colorless (Ross Jr, 2016).

The determination of the freezing protocol is a crucial step for the success of the procedure and the viability of the sample. It depends on some factors, such as the nature of the cellular material, type and concentration of cryoprotective agents (CPAs), freezing speed, defrost speed, the time of exposure of the structure to the cryoprotective solution, and others (Santin *et al.*, 2009). Among these factors, the freezing speed and the type/concentration of cryoprotectant solutions are strongly correlated, because higher cooling speeds tend to cause cell disruption due to the generation of ice crystals, and it's opposite, cell dehydration. Thus, cryoprotective solutions play an important role in reducing the damage caused during the cryopreservation process (Silva *et al.*, 2017).

However, some cryoprotectants are not entirely inert, as the Dimethylsulfoxide (DMSO) widely used in cryopreservation activities. According to studies, DMSO has high toxicity and cannot be applied to patients in high doses, having a high potential to cause some side effects previously reported in the literature, such as nausea, vomiting, diarrhea, renal failure, bradycardia, hypertension, pulmonary edema, among other problems. In order to mitigate these effects, actions like cell washing to remove DMSO, fractional infusion, decreasing the percentage of cryoprotectant to less than 10% and replacing it for sugars, sugar alcohols, specialized polymers and small molecules have been studied, accordingly to Santos *et al.* (2003), Jong *et al.* (2019) and Weng and Beauchesne (2020).

Among the conventional methods of cryopreservation, stands out the programmed freezing protocol, which is widely used in the freezing of embryos, stem cells and tissues. In this method, the samples are frozen in a programmable cryocooler, as shown in Fig. 1 for example, with a good viability index, through the slow and step freezing, using low cooling speeds together with cryoprotectant solutions.



Figure 1. Programmable cryocooler CryoMed TM (ThermoFisher, 2021).

In order to improve the performance of cryopreservation protocols, several studies have been carried out to replace the low freezing speeds traditional protocols for alternative protocols with high freezing speeds. In the methods of cryopreservation by vitrification, the biological sample undergoes a direct transition from the liquid state to a vitrified and amorphous state without the occurrence of crystallization, with high practicality, low cost and time of operation (Santin *et al.*, 2009).

Nevertheless, the development of ultra-fast freezing systems by vitrification is quite complex, requiring specialized laboratories and equipment, large amounts of experimental validation tests, resulting in a high cost of time and money during the project. In this way, through the computational fluid dynamics (CFD) it is possible to make less expensive the study and development of these systems, besides being possible to evaluate with more details the physical phenomena involved during the samples freezing.

Thus, this work will carry out a brief review of the ultra-fast freezing process by vitrification available in the literature. The main protocols will be numerically reproduced in order to study the physical phenomena involved during the freezing, such as cooling rates, solidification process and influence of the biological material sizes and the contact angle with surface.

2. ULTRA-FAST FREEZING METHODS

Research has been carried out in order to optimize the relationship between cryoprotective solution, sample viability and freezing rate, through the improvement of existing protocols and the development of new concepts of ultra-fast freezing. The following sections will introduce the most common methods of ultra-fast freezing by vitrification presented in the literature.

2.1 Open Pulled Straw (OPS)

Vajta *et al.* (1998), developed the OPS vitrification protocol (Open Pulled Straw) to work initially with bovine embryos, as showed in Fig. 2.

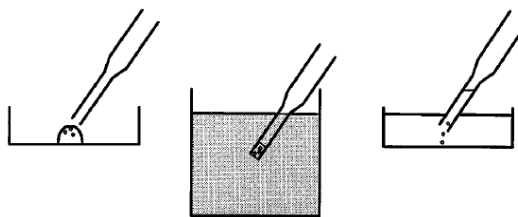


Figure 2. OPS vitrification method (Vajta *et al.*, 1998).

This method consists of collect the embryos through a tube by the capillarity effect and then submerge them in a container filled with liquid nitrogen, until the suspended cells inside the tube are completely frozen. Through the OPS method, cooling speeds above 20,000 °C/min can be achieved with a short contact with cryoprotective agents, less than 30 s to a temperature of -180 °C, minimizing the toxic and osmotic effects of cryoprotective substances.

2.2 Thin Film Evaporation

According to Su *et al.* (2018), the greatest impediment to achieve higher cooling rates is due to the liquid nitrogen vaporization on the surface of the samples when immersed in it, as in the EM grip, OPS and Cryoloop methods. In this region, a vapor film occurs, thus limiting the heat transfer coefficient between the sample surface and liquid nitrogen to values lower than $1,000 \text{ W/m}^2\text{K}$, with a typical cooling rate around 25,000 °C/min, due to low thermal conductivity of the vapor film. In order to solve this problem, the authors developed an ultra-fast vitrification method of cell cryopreservation using a thin evaporation film, as shown in Fig. 3.

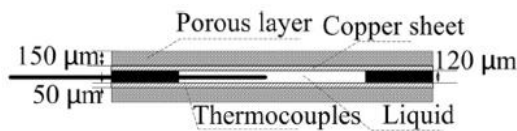


Figure 3. Ultra-fast vitrification by thin vapor film (Su et al., 2018).

In this system, the stored liquid nitrogen is dispersed in a porous layer of copper (microstructured), through the capillarity effect, filling the empty spaces between the microparticles. Then, the liquid nitrogen forms a liquid thin film on the microstructured surface evaporating rapidly due to capillarity and peeling pressure effects. In account of this ultra-fast evaporation and heat absorption, the authors achieved high cooling rates in the order of 150,000 °C/min (reducing the temperature from 10 °C to -180 °C in approximately 0.074 s). It was also possible to obtain a heat transfer coefficient in the order of 10^6 W/m²K, together with a considerable reduction in cryoprotective agents.

In another work, Su *et al.* (2019) compared the thin film evaporation method (TFE) with OPS method, in the freezing of hamster ovary cells. The authors found that using the TFE method it is possible to achieve higher cooling rates than OPS method, due to the high heat flow in the region (315,3 W/m² to 139,4 W/m²). It was also found a higher cell survival rates, because of the higher heat transfer coefficient than in the OPS case (1,965 W/m² °C and 904 W/m² °C, for TFE and OPS, respectively).

2.3 Superflash Freezing (SFF) by Dripping

Akiyama *et al.* (2019), developed a system for the cryopreservation of mammalian cells by ultra-fast freezing, called Superflash Freezing (SFF) without the use of cryoprotective agents. The authors applied numerical simulations to estimate cooling rates using a commercial software (COMSOL®), with experimental validation. For this purpose, a droplet printing technique was used in which microdroplets are deposited on a surface at extremely low temperature immersed in a gaseous phase resulting from the evaporation of liquid nitrogen. Thus, it was possible to obtain extremely high cooling speeds, reaching a state close to vitrification, as shown in Fig. 4.

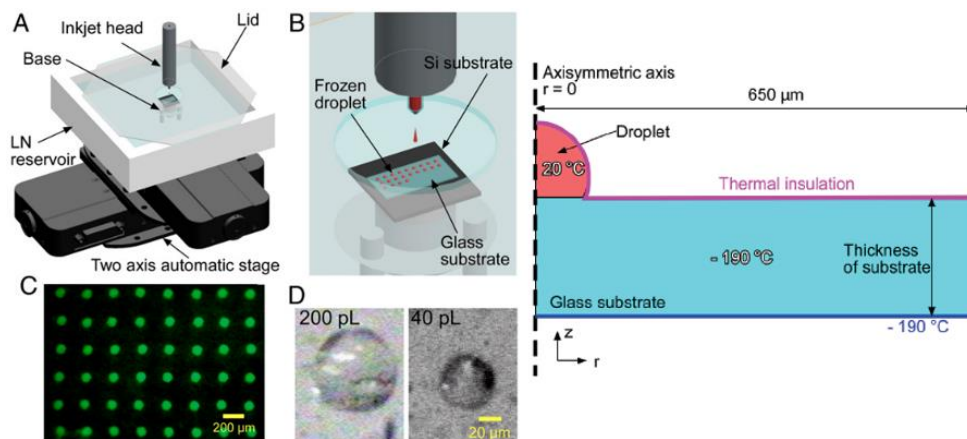


Figure 4. Superflash freezing method by dripping - adapted from Akiyama et al. (2019).

Through this approach, the authors achieved cooling rates around 3.7×10^4 °C/s, varying the substrate thickness (150 μm and 5 μm) and the drip nozzle diameter (60 μm and 40 μm). It was used droplets with approximately 200 pL and 40 pL in volume. The authors compared the SFF (cryoprotectant-free) ultra-fast freezing method with a conventional low freezing speed protocol (10% DMSO by volume). They found that the SFF protocol showed high cell viability, especially for small cells, such as sperm and thrombocytes, with future applications in pluripotent stem cells and hemocytes for blood transfusion.

Marchesi *et al.* (2005) also studied the drip vitrification process (without cryoprotectants) through a CFD analysis via Ansys Fluent®, using a model considering the conductive heat transfer combined with the solidification phase change. The objective of this study was to evaluate the thermal viability of the method and the influence of the thermo-physical parameters involved. Figure 5 shows the simulation conditions of the applied drip vitrification process.

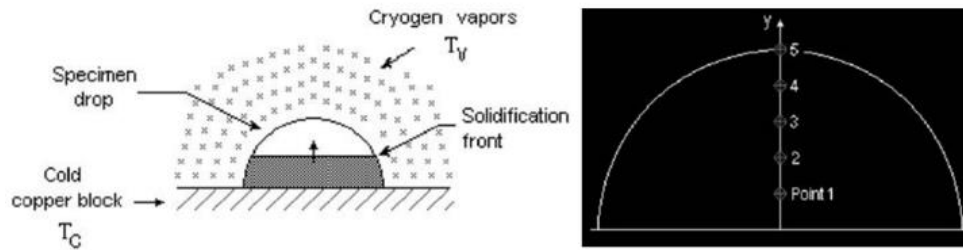


Figure 5. Numerical domain used in computer simulation (Marchesi et al., 2005).

The authors evaluated the variation of the sample diameter (droplet), by collecting temperature at five different radial points, using two types of refrigerant fluid (liquid nitrogen and liquid helium). The influence of the vapor temperature in relation to the substrate temperature was also studied. It was verified that the cooling rate within the sample has spatial and temporal dependence, varying according to the position inside the sample. In addition, it was observed that the parameters that have the greatest influence on the variation of the cooling rate are the temperature and the thickness of the substrate (order of 100x), with cooling rates $>150,000$ °C/s.

3. MATERIALS AND METHODS

In this work, numerical simulations (CFD) of the drip freezing protocol were performed using the commercial software ANSYS Fluent®, analyzing the cooling rate, solidification curve and droplet characteristics, such as size, shape and contact angle. The domain is two-dimensional, formed by a droplet of water deposited on a glass surface, as shown in Figure 6. Three geometries with different contact angles with the substrate were analyzed, $\theta = 90^\circ$, $\theta = 135^\circ$ and $\theta = 45^\circ$, respectively, keeping constant the droplet volume of $20 \mu\text{L}$, as used by O'Neill *et al.* (2019).

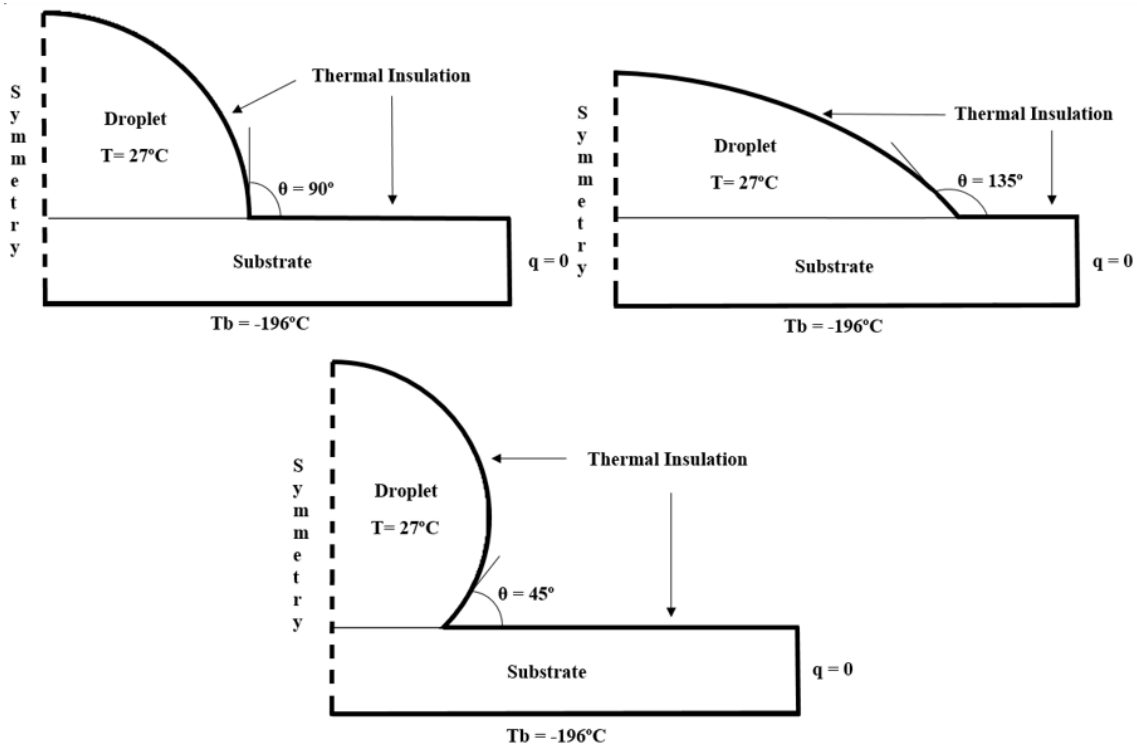


Figure 6. Numerical domain and boundary conditions.

The droplet and substrate surfaces in contact with the environment were considered thermally insulated, with heat transfer only at the drop-substrate interface. The substrate base is maintained at a constant temperature of -196°C and the droplet is simulated initially with a temperature of 27°C . The domain around the droplet is considered five times larger than the droplet diameter, as applied by Marchesi *et al.* (2005).

The thermal properties of the droplet and the substrate were considered temperature dependent properties and were obtained through the Engineering Equation Solver (EES) library varying their values according to Table 1.

Table 1. Thermal properties of water and glass.

Temperature [K]	Water				Glass	
	Density [kg/m ³]	Specific heat [J/kg K]	Thermal conductivity [W/m K]	Viscosity [kg/m s]	Specific heat [J/kg K]	Thermal conductivity [W/m K]
77	934.3	0.7427	2.786	-	0.8241	0.4175
93	933.8	0.8447	2.729	-	1.094	0.518
123	932.3	1.04	2.623	-	1.408	0.6599
153	930.3	1.242	2.516	-	1.656	0.7849
183	927.7	1.449	2.41	-	1.835	0.8828
213	924.6	1.663	2.303	-	1.979	0.9707
243	920.9	1.882	2.197	-	2.078	1.046
263	918.1	2.056	2.125	-	2.111	1.087
273	1000	4.228	0.5475	0.001793	2119	1.106
278	1000	4.2	0.5576	0.001519	2.123	1.115
283	999.7	4.188	0.5674	0.001307	2.127	1.125
288	999.1	4.184	0.577	0.001138	2.131	1.134
293	998.2	4.183	0.5861	0.001002	2.135	1.143
298	997.1	4.183	0.5948	0.0008905	2139	1.153
303	995.7	4.183	0.603	0.0007977	2.14	1.161

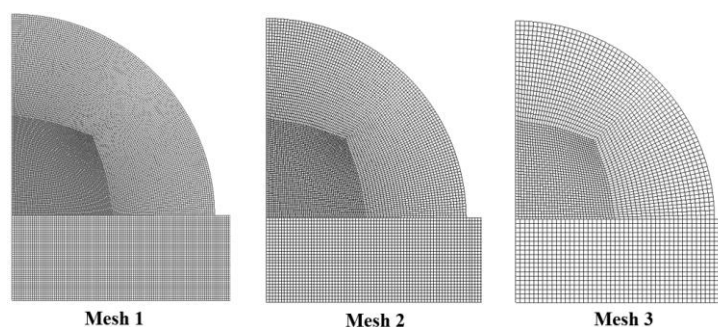
The pure solvent melting heat (enthalpy of fusion) of water is a constant value of 333.6 kJ/kg with the phase change temperature from liquid to solid around 273 K (0 °C). The glass density is temperature independent with a value of 2,225 kg/m³.

3.1 Computational Mesh Analysis

The computational mesh analysis was performed using the Grid Convergence Method (GCI) presented by Celik *et al.* (2008), where 3 meshes were evaluated with a mesh refining ratio (r) of 1.5 with 35,893, 16,269 and 7,278 elements, respectively, using the liquid mass fraction (β) as a refining parameter. The chosen mesh was the most refined, with a GCI of 1.28%, below the acceptable 5% in the literature, indicating that the mesh is able to reproduce the physical phenomena involved with good accuracy. Table 2 shows the mesh quality parameters used in this work and Fig. 7 shown the mesh appearance.

Table 2. Mesh quality information.

Mesh	Element size [m]	N° of elements	Orthogonal quality [-]	Skewness [-]
1	2.381×10^{-5}	35893	0.99271	0.00349
2	3.571×10^{-5}	16269	0.99263	0.00358
3	5.357×10^{-5}	7278	0.99264	0.00362

Figure 7. Mesh appearance for refine ratio $r = 1.5$.

3.2 CFD Setup and Governing Equations

The setup of the numerical simulations for droplet vitrification was performed using the Solidification model of the ANSYS Fluent®, wherein the energy equation is written in terms of enthalpy, as shown in Eq. 1. It was simulated cases considering a transient formulation during 50 s, with a time step size of 0.05 s and with a viscous model defined as laminar.

$$\frac{\partial}{\partial t}(\rho H) + \nabla \cdot (\rho \vec{v} H) = \nabla \cdot (k \nabla T) + S \quad (1)$$

where k is the thermal conductivity, ρ is the density, \vec{v} is the fluid velocity, S is the source term and H is the enthalpy of the material, calculated through the sensible enthalpy, h , and the latent heat, ΔH , according to Eq. 2, 3 and 4.

$$H = h + \Delta H \quad (2)$$

$$h = h_{ref} + \int_{T_{ref}}^T c_p dT \quad (3)$$

$$\Delta H = \beta L \quad (4)$$

where h_{ref} and T_{ref} are the reference enthalpy and temperature of reference, respectively, c_p is the specific heat at constant pressure, β is the liquid fraction and L is the latent heat of the material. The continuity (Eq. 5) and momentum (Eq. 6) equations are given as:

$$\frac{\partial \rho}{\partial t} + \nabla \cdot (\rho \vec{V}) = 0 \quad (5)$$

$$\frac{\partial \rho \vec{V}}{\partial t} + \nabla \cdot (\rho \vec{V} \vec{V}) = -\nabla p + \nabla \cdot (\mu \nabla \vec{V}) + \rho \vec{g} + S \quad (6)$$

where S is the source term calculated for Eq. 7, that use the mush zone constant, A_{mush} , volume liquid fraction, β , and ε that is a small number to avoid division by zero:

$$S = \frac{(1 - \beta)^2}{(\beta^3 + \varepsilon)} A_{mush} \cdot \vec{V} \quad (7)$$

The discretization method to solve the pressure-velocity coupling was set as SIMPLE, with a *second order* algorithm to solve pressure, momentum, energy and transient formulation.

4. RESULTS AND DISCUSSION

From the computer simulations performed, it was possible to obtain the droplet cooling curve and droplet solidification behavior varying the contact angle $\theta = 45^\circ$, $\theta = 90^\circ$ and $\theta = 135^\circ$. Figure 8 shows the influence of the contact angle on the cooling curves and on the solidification behavior, where greater contact angles (hydrophilic surfaces) present higher cooling rates and solidification rates. The droplet with $\theta = 135^\circ$ froze completely before 6 s, less than a half of the droplet with $\theta = 45^\circ$, and reach a temperature of 80 K in less than 20 s, while for $\theta = 45^\circ$ the time was more than 40 s.

The average cooling rate until the complete solidification point for each slope can be observed, where $\theta = 45^\circ$ has an average cooling rate of 335.277 K/min, $\theta = 90^\circ$ has 655.643 K/min and $\theta = 90^\circ$ has 1132.55 K/min. This is due to the relationship between wettability and the contact angle with the droplet-substrate interface area, where greater contact angles result in larger interface areas and consequently greater heat transfer flow. This analysis can also be seen by the temperature contours at different time points, as shown in Fig. 9.

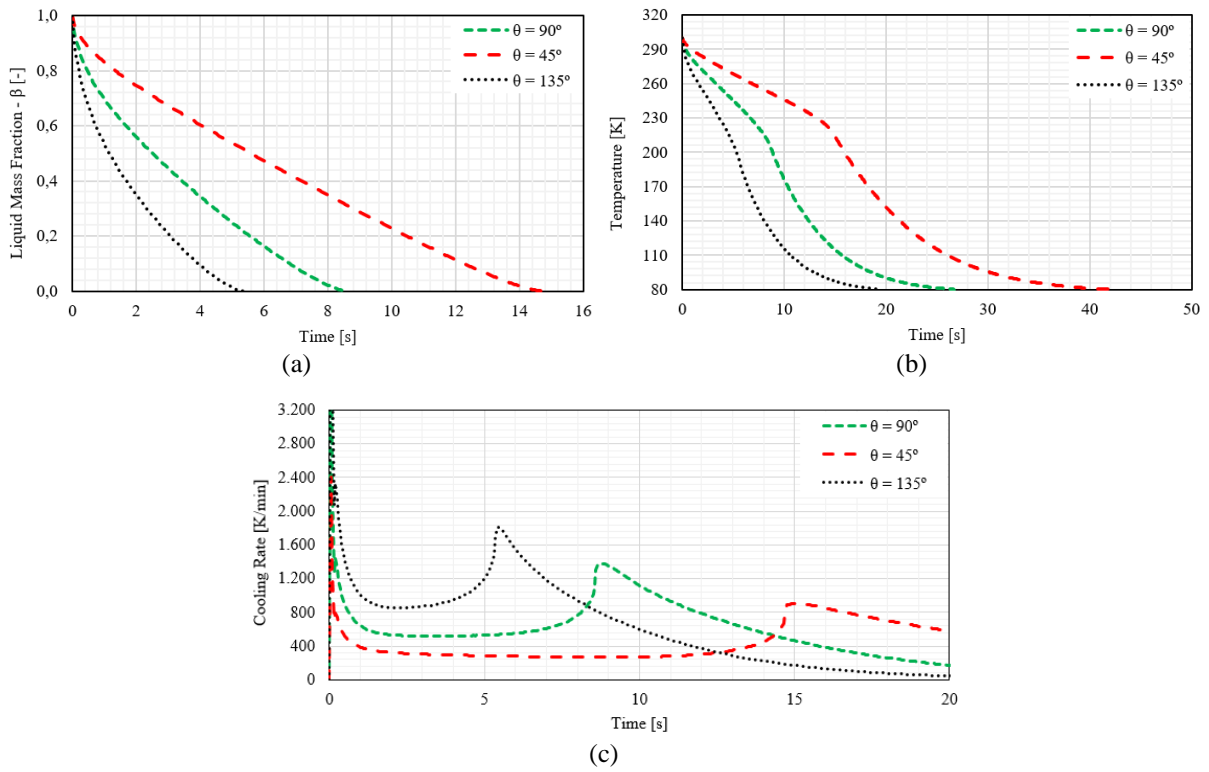


Figure 8. Solidification (a), temperature (b) and cooling rate (c) curves of the droplet during vitrification process.

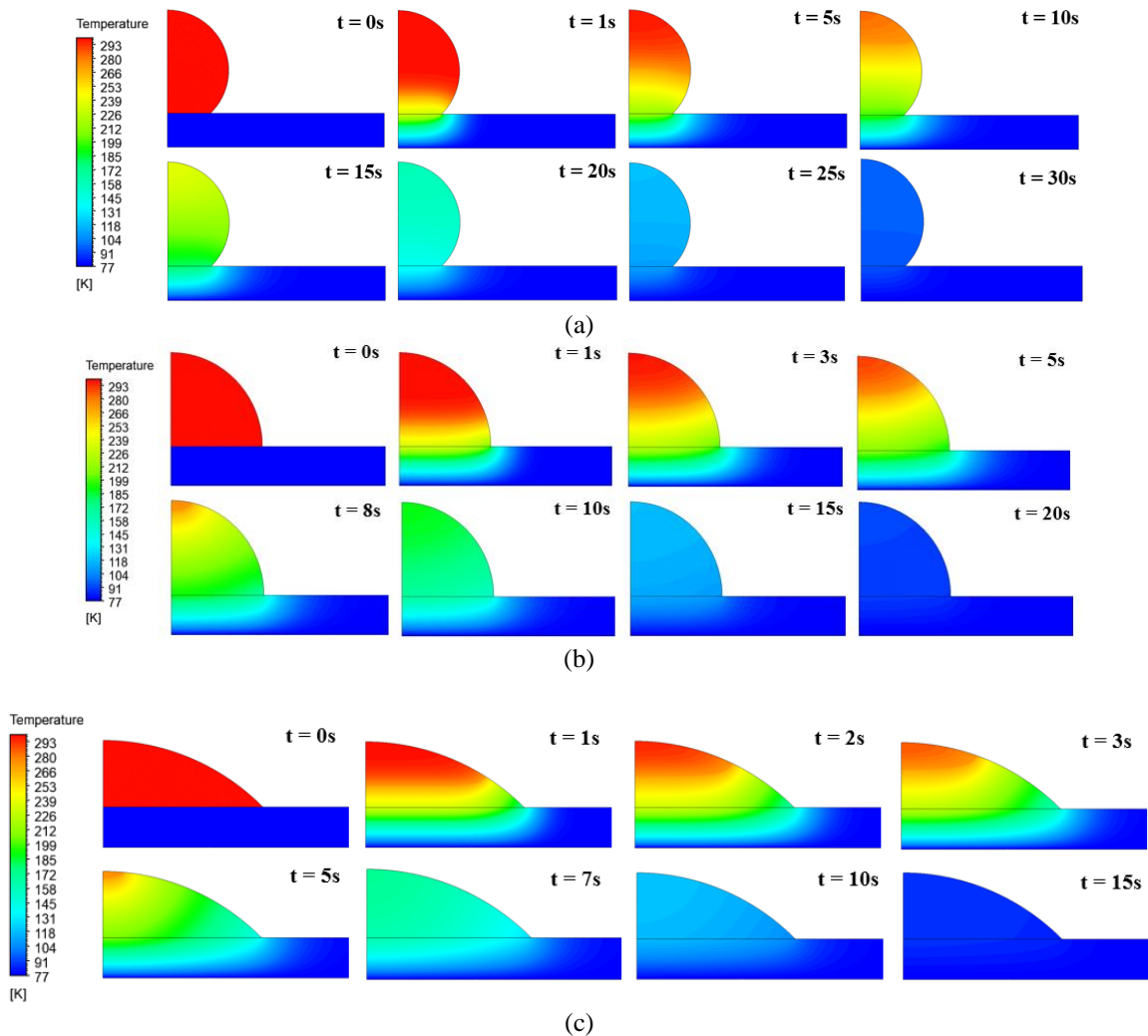


Figure 9. Contours of temperature for (a) $\theta = 45^\circ$, (b) $\theta = 90^\circ$ and (c) $\theta = 135^\circ$ in different times.

The information obtained in Fig. 8 can be confirmed through the solidification contours of the droplet, analyzing the variation of the mass fraction of liquid over time, showed in Fig. 10.

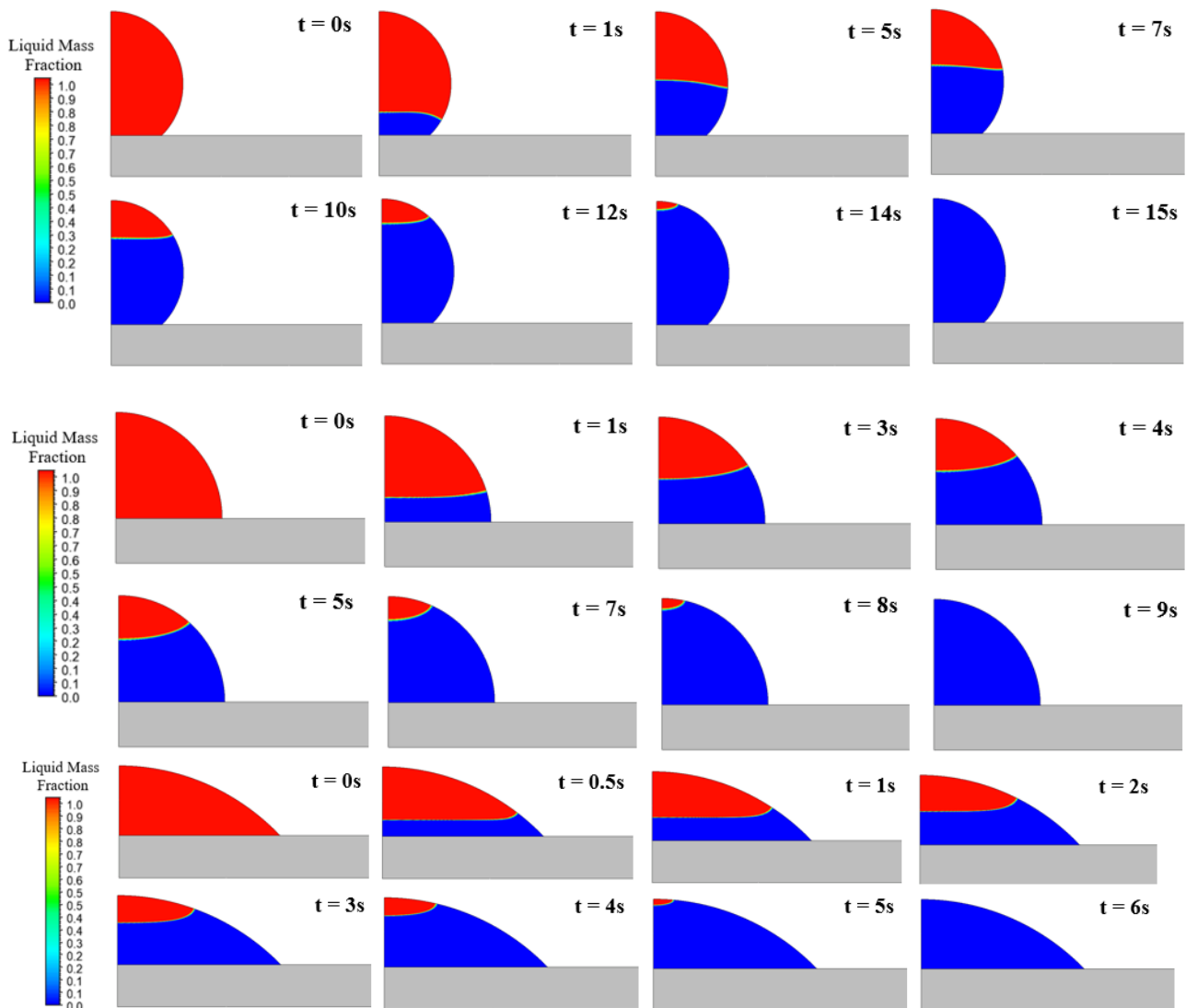


Figure 10. Contours of liquid mass fraction for $\theta = 45^\circ$, $\theta = 90^\circ$ and $\theta = 135^\circ$.

The results presented in this work show the influence of the droplet characteristics on the solidification cooling rate, in which hydrophilic surfaces with $\theta > 90^\circ$ provide a greater heat transfer flow between the sample and the substrate. The cooling rate curve showed a different behavior up to the point of total freezing $\beta = 0$ (an increment of the cooling rate near the solidification point) diverges from the results found in the literature, such as in Marchesi *et al.* (2005) and Jiao *et al.* (2006). This phenomenon may be related to the volume of the droplet, where larger volumes lead to lower cooling rates and greater probability of crystallization inside the sample.

The next step of this study will be to carry out the experiment to investigate the inconsistencies found in the cooling curve in relation to the literature. It is also intended to evaluate the influence of the amount of cryoprotectant solutions (CPA) on the cooling and crystallization curves. Finally, in future works they will investigate the numerical and experimental vitrification of different types of biological samples, for example, semen and stem cells from blood.

5. CONCLUSION

The vitrification process of biological materials is a very interesting and complex area, as it involves many variables and physical phenomena, which are often impractical to obtain experimentally. Using CFD computer simulations, was possible to analyze a dripping vitrification system with great wealth of details, generating cooling and solidification curves, as well as temperature contours for different time instants.

Three contact angle values were evaluated, $\theta = 45^\circ$, $\theta = 90^\circ$ and $\theta = 135^\circ$, keeping the droplet volume constant in order to obtain the influence of this parameter on the freezing speed. It was found that surfaces with a high level of wettability, i.e., with a contact angle greater than 90° , present higher rates of cooling and solidification, where $\theta = 135^\circ$

obtained a cooling rate of 1132.55 K / min, almost four times greater than the case with a contact angle $\theta = 45^\circ$. This is due to the increase in the contact area of the droplet with the substrate for high contact angle values, thus generating greater heat flow in the droplet-substrate interface.

An interesting point to be investigated in future works is the behavior of the cooling rate close to the moment when the complete droplet solidification occurs, with an increase in the cooling values. Thereby, new simulations and experimental tests will be performed to treat this phenomenon with greater emphasis. In the general context, the CFD results presented in this study are in agreement with those found in the literature, being an excellent tool to study and investigate phenomena involving vitrification processes.

6. AUTHORIZATIONS/ RECOGNITION

The authors are the only responsible for the printed material included in this paper.

Acknowledgements

The first author of this article would like to thank CNPQ for their grant within the CNPQ/DAI - Unisinos project.

7. REFERENCES

- Akiyama, Y., Shinose, M., Watanabe, H., Yamada, S. and Kanda, Y., 2019. "Cryoprotectant-free cryopreservation of mammalian cells by superflash freezing". In *Proceedings of the National Academy of Sciences of the United States of America*, Vol. 116, No. 16, pp. 7738–7743.
- Cerdeira, J., Sánchez-Calabuig, M.J., Pérez-Gutiérrez, J.F., Híjon, M. Castaño, C. and Santiago-Moreno, J., 2020. "Cryopreservation effects on canine sperm morphometric variables and ultrastructure: comparison between vitrification and conventional freezing". *Cryobiology*, <https://doi.org/10.1016/j.cryobiol.2020.03.007>.
- Dalman, A., Farahani, N.S.D.G., Totonchi, M., Pirjani, R., Ebrahimi, B. and Valorjerdi, M.R., 2017. "Slow freezing versus vitrification technique for human ovarian tissue cryopreservation: an evaluation of histological changes, WNT signaling pathway and apoptotic genes expression". *Cryobiology*, Vol. 79, pp. 29–36.
- Jiao, A., Han, X., Critser, J. K., & Ma, H. 2006. "Numerical investigations of transient heat transfer characteristics and vitrification tendencies in ultra-fast cell cooling processes". *Cryobiology*, 52(3), 386–392. <https://doi.org/10.1016/j.cryobiol.2006.01.009>
- Jong, K. S., Hui, L.Y., Yu, C.M., Ki, S.Y., Kim, S.H. and Pak, H.H., 2020. "The impact of cryoprotective media on cryopreservation of cells using loading trehalose". *Cryobiology*, Vol. 92, pp. 258-259.
- Le, M. T., Nguyen, T.T.T., Nguyen, T.T., Nguyen, V.T., Nguyen, T.T.A., Nguyen, V.Q.H. and Cao, N.T., 2019. "Cryopreservation of human spermatozoa by vitrification versus conventional rapid freezing: effects on motility, viability, morphology and cellular defects". *European Journal of Obstetrics and Gynecology and Reproductive Biology*, Vol. 234, pp. 14–20.
- Li, Y-X., Zhou, L., Lv, M-Q., Ge, P., Liu, Y-C. and Zhou, D-X., 2019. "Vitrification and conventional freezing methods in sperm cryopreservation: a systematic review and meta-analysis". *European Journal of Obstetrics and Gynecology and Reproductive Biology*, Vol. 233, pp. 84–92.
- Marchesi, R., Maffè, M. and Moraschi, M., 2005. "Computational fluid dynamics analysis of cell cooling process". *Cell Preservation Technology*, Vol. 3, No. 4, pp. 229–237.
- O'Neill, H. C., Nikoloska, M., Ho, H. T., Doshi, A., & Maalouf, W. 2019. "Improved cryopreservation of spermatozoa using vitrification: comparison of cryoprotectants and a novel device for long-term storage". *Journal of Assisted Reproduction and Genetics*, 36(8), 1713–1720. <https://doi.org/10.1007/s10815-019-01505-x>
- Ross, R. G., 2016. *Refrigeration Systems for Achieving Cryogenic Temperatures*. CRC Press, Taylor & Francis, Boca Raton.
- Santin, T. R., Blume, H., Mondadori, R. G., 2009. "Conservação de embriões – metodologias de vitrificação". *Veterinária e Zootecnia*, Vol. 16, No. 4, pp. 561-574.
- Santos, N. C., Figueira-Coelho, J. , Martins-Silva, J. and Saldanha, C., 2003. "Multidisciplinary utilization of dimethyl sulfoxide: pharmacological, cellular, and molecular aspects". *Biochemical Pharmacology*, Vol. 65, No. 7, pp. 1035-1041.
- Silva, A. A. R.; Rodrigues, C. G. and Silva, M. B. da., 2017. "Avanços tecnológicos na criopreservação de células-tronco e tecidos, aplicados à terapia celular". *Revista da Biologia*, Vol. 17, No. 1, pp. 13-18.
- Su, F., Zhao, N., Deng, Y. and Ma, H., 2018. "An ultrafast vitrification method for cell cryopreservation". *Transactions of the ASME Journal of Heat Transfer*, Vol. 140, No. 1, pp. 1-4, 2018.
- Su, F., Fan, Y., Xu, H., Zhao, N., Ji, Y. and Ma, H., 2019. "Ultra-fast vitrification experiment of mamster ovary cells utilizing thin film evaporation". In *Proceedings of the 25th IIR International Congress of Refrigeration – ICR 2019*. Montreal, Canada.
- Thermofisher, 2021. "CryoMed™ Controlled-Rate Freezers". Available from: <https://www.thermofisher.com/order/catalog/product/7450#/7450>. Accessed in: February 12, 2021.

- Vajta, G., Holm, P., Kuwayama, M., Booth, P.J., Jacobsen, H., Greve, T. and Callesen, H., 1998. "Open pulled straw (OPS) vitrification: A new way to reduce cryoinjuries of bovine ova and embryos". *Molecular Reproduction and Development*, Vol. 51, No. 1, pp. 53-58.
- Weng, L. and Beauchesne, P. R., 2020. "Dimethyl sulfoxide-free cryopreservation for cell therapy: A review. *Cryobiology*". Vol. 94, pp. 9-17.